

3D nano crystalline metal-organic framework materials improve output performance of triboelectric nanogenerator

Kexin Gao^{a,*} Junshuai Chen,^{a,*} Mengting Zhao,^a Rentang Hu,^a Shiheng Chen,^a Xiaojing Xue,^b Zhichao Shao,^{*,a} and Hongwei Hou^{*,b}

[^a] Center for Advanced Materials Research, Zhongyuan University of Technology, Zhengzhou 450007, P. R. China.

[^b] College of Chemistry, Zhengzhou University, Zhengzhou, Henan, 450001, P. R. China

[+] These authors contributed equally to this work.

E-mail address: *shaozhichao@zut.edu.cn, houhongw@zzu.edu.cn*

Supporting Information

Fig. S1 Chemical structure of twisted organic ligand.

Fig. S2 The possible modes of charge transfer in Cd-MOF.

Fig. S3 PXRD pattern of Cd-MOF.

Fig. S4 XPS full spectra of Cd-MOF.

Fig. S5 I_{SC} of Cd-MT at 1 Hz.

Fig. S6 I_{SC} of Cd-MT at 2 Hz.

Fig. S7 I_{SC} of Cd-MT at 4 Hz.

Fig. S8 I_{SC} of Cd-MT at 6 Hz.

Fig. S9 I_{SC} of Cd-MT at 8 Hz.

Fig. S10 V_0 of Cd-MT at different frequency.

Fig. S11 V_0 of Cd-MT at 5 Hz.

Fig. S12 Effect of temperature on output performance in Cd-MT.

Fig. S13 SEM images of Cd-MOF on the Cu layer.

Fig. S14 EDS elemental analysis of PVDF layer.

Fig. S15 High-definition digital and SEM images of PVDF layer.

Fig. S16 EDS images of PVDF layer

Fig. S17 Uv-vis spectra of Cd-MOF.

Fig. S18 Tauc plot of Cd-MOF.

Fig. S19 I_{SC} of Cd-MT through a rectifier bridge.

Fig. S20 Charging of 100 μF capacitor using Cd-MT at 5Hz.

Table S1 Crystallographic data and structure refinement details for Cd-MOF.

Table S2 Selected bond lengths (\AA) and bond angles (deg) for Cd-MOF crystal structure description.

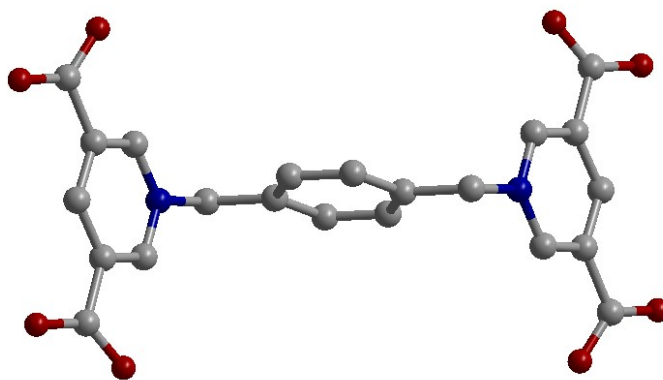


Fig. S1 Chemical structure of twisted organic ligand.

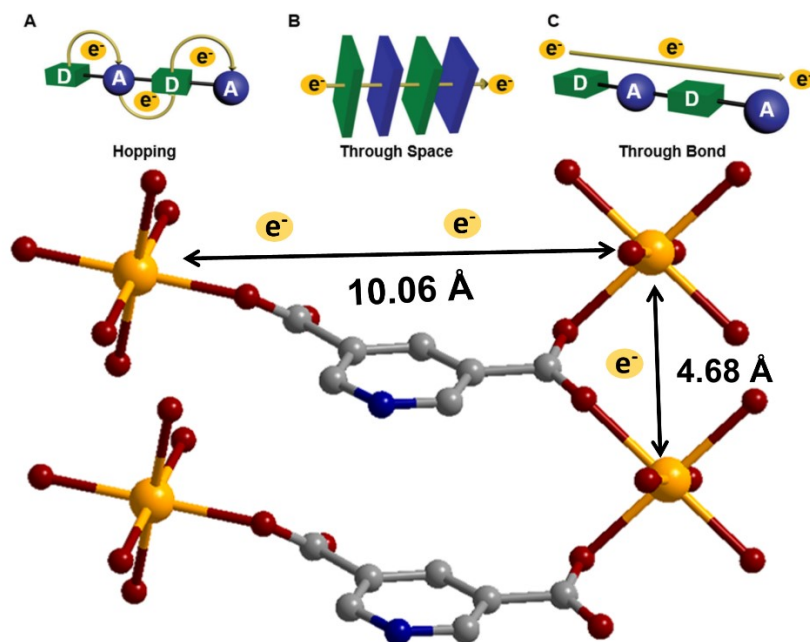


Fig. S2 The possible modes of charge transfer in Cd-MOF.

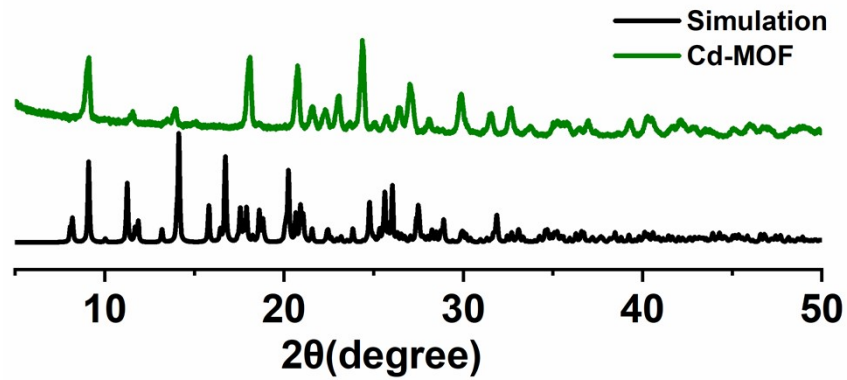


Fig. S3 PXRD pattern of Cd-MOF.

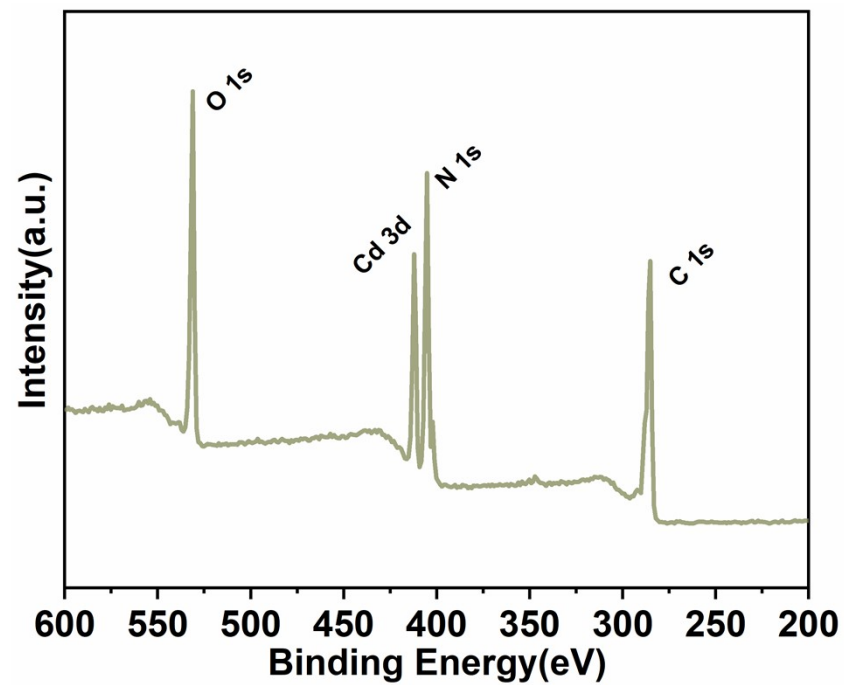


Fig. S4 XPS full spectra of Cd-MOF.

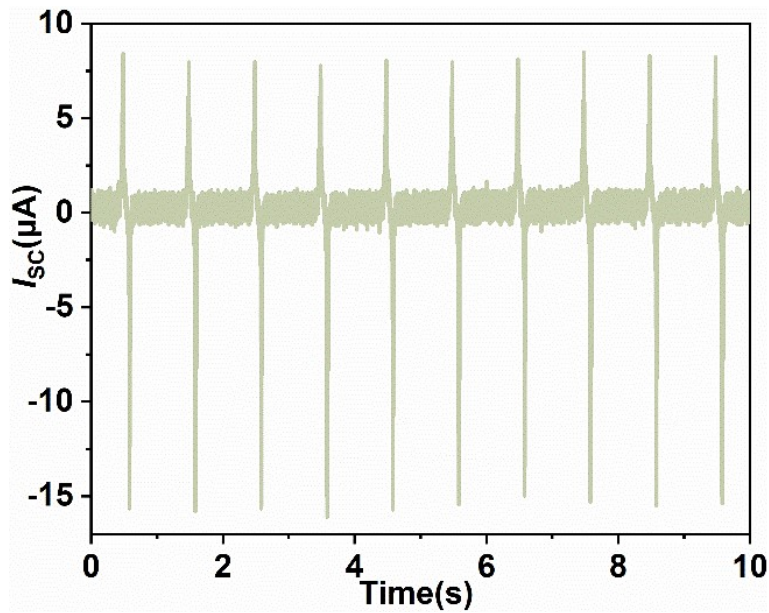


Fig. S5 I_{sc} of Cd-MT at 1 Hz.

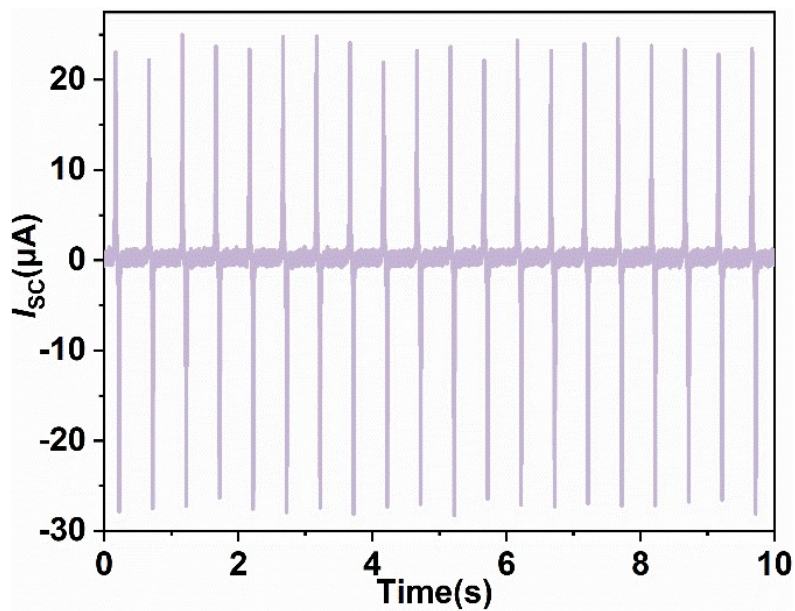


Fig. S6 I_{sc} of Cd-MT at 2 Hz.

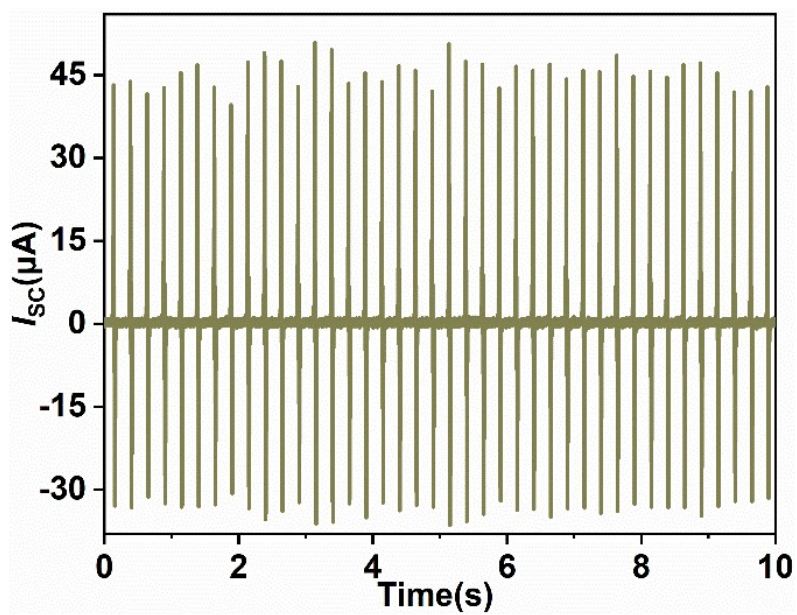


Fig. S7 I_{sc} of Cd-MT at 4 Hz.

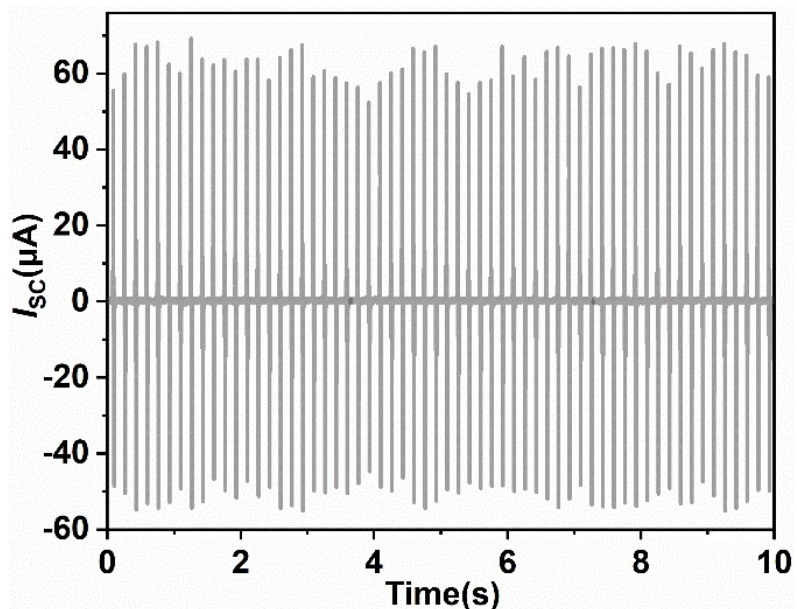


Fig. S8 I_{sc} of Cd-MT at 6 Hz.

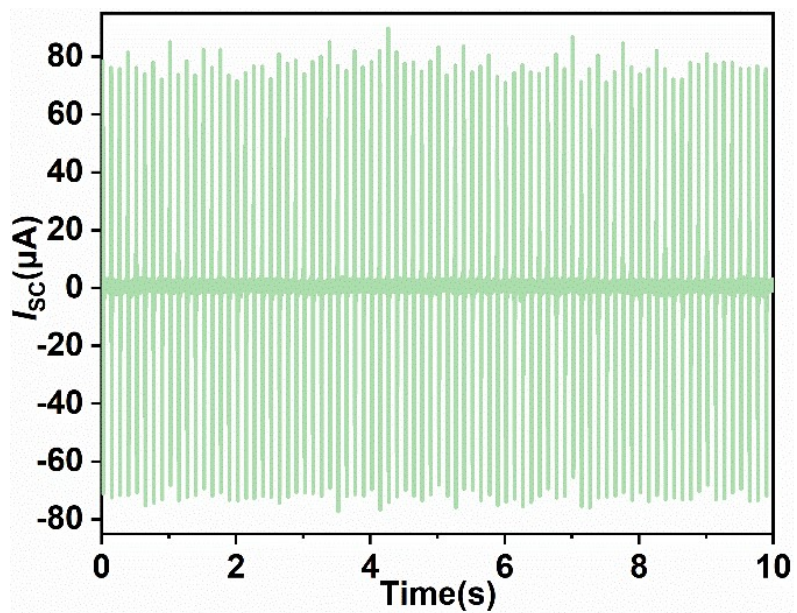


Fig. S9 I_{SC} of Cd-MT at 8 Hz.

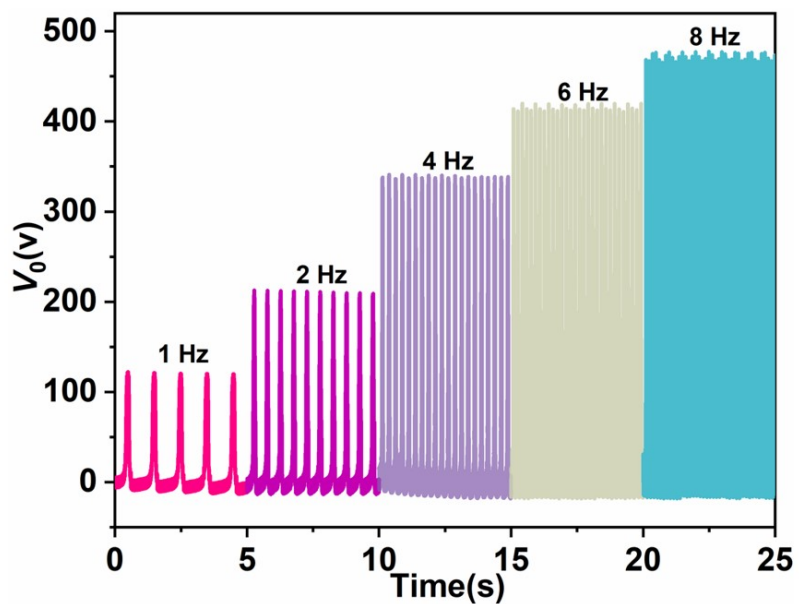


Fig. S10 V_0 of Cd-MT at different frequency.

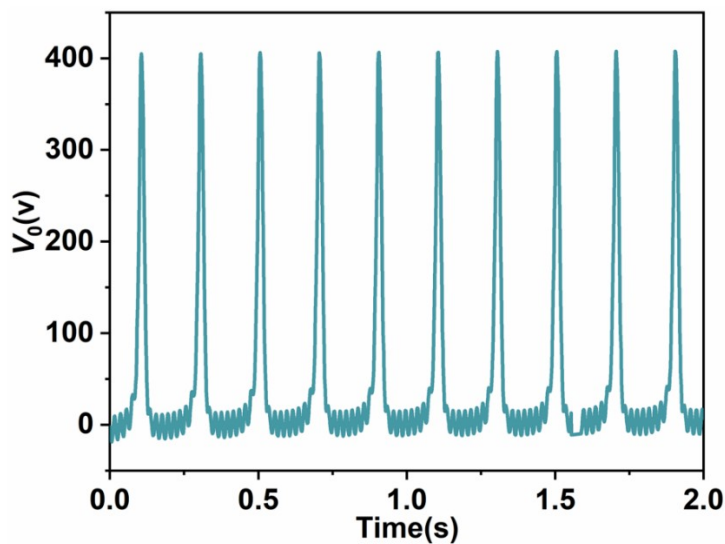


Fig. S11 V_0 of Cd-MT at 5 Hz.

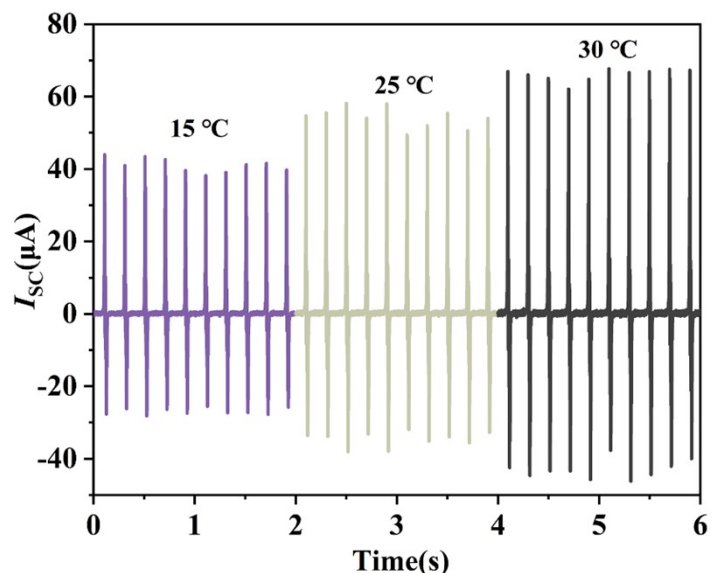


Fig. S12 Effect of temperature on output performance in Cd-MT.

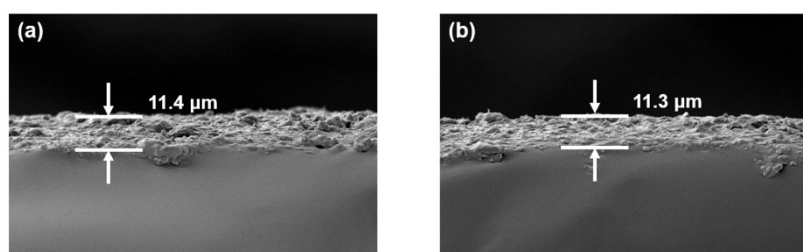


Fig. S13 SEM images of Cd-MOF on the Cu layer (a) before and (b) after testing.

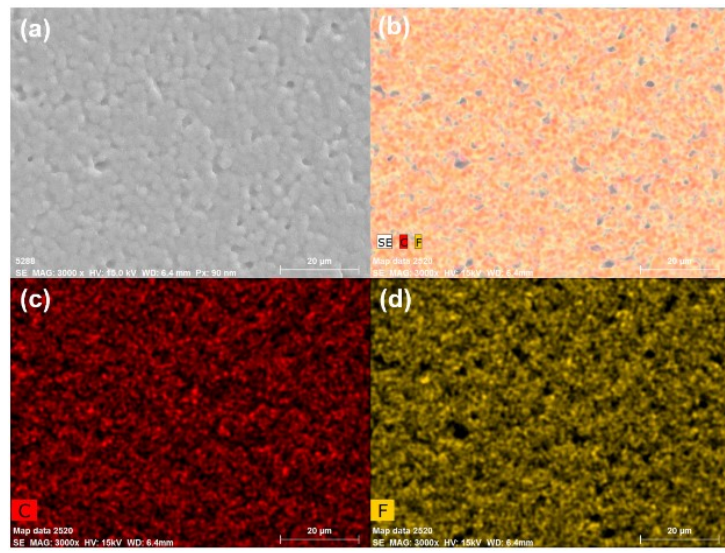


Fig. S14 EDS elemental analysis of PVDF layer.

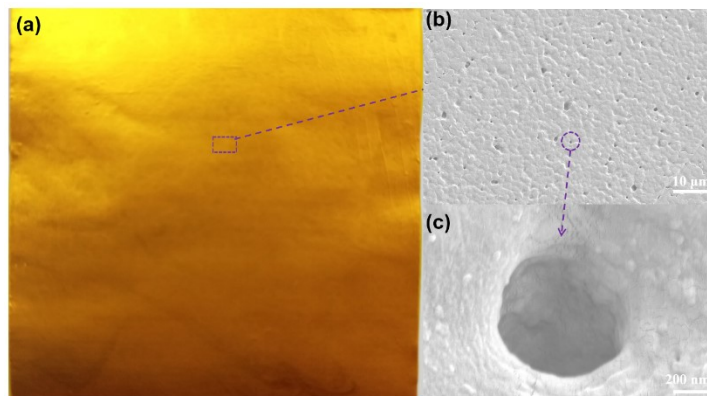


Fig. S15 High-definition digital and SEM images of PVDF layer.

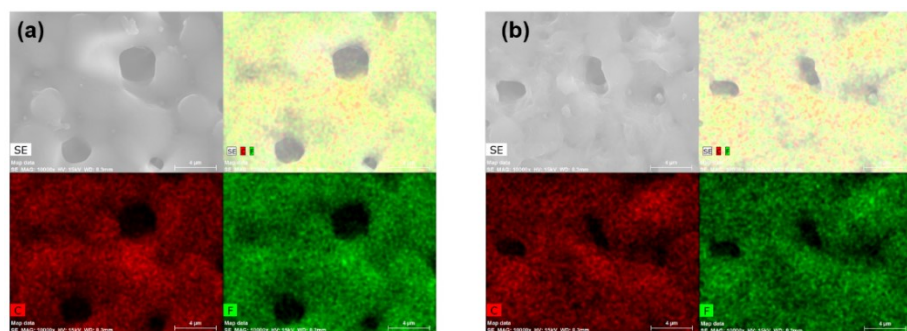


Fig. S16 EDS images of PVDF layer (a) before and (b) after testing.

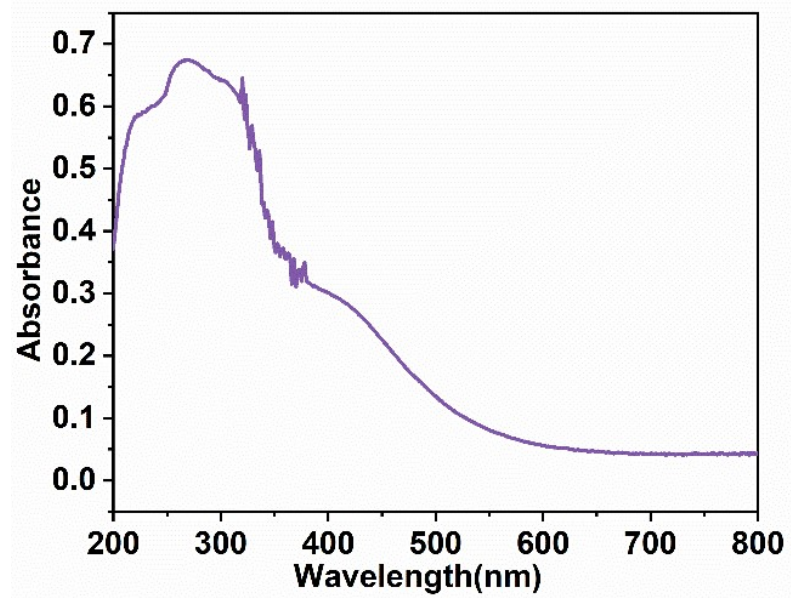


Fig. S17 Uv-vis spectra of Cd-MOF.

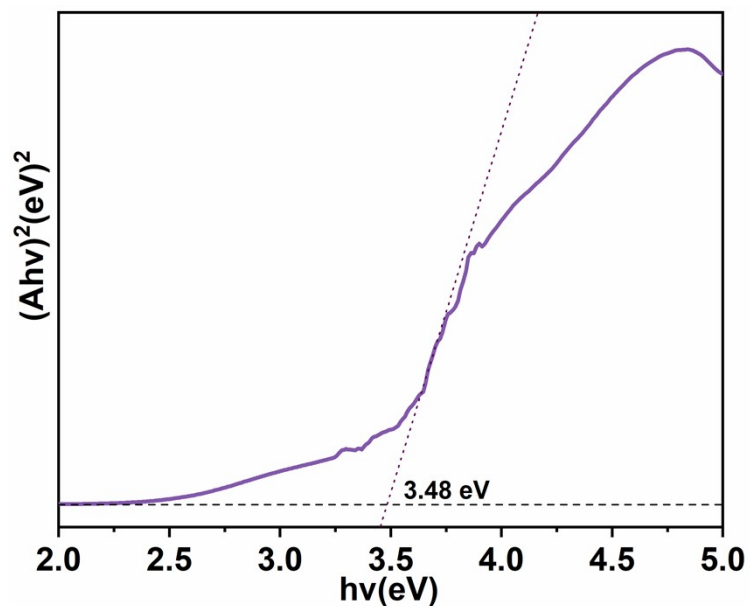


Fig. S18 Tauc plot of Cd-MOF.

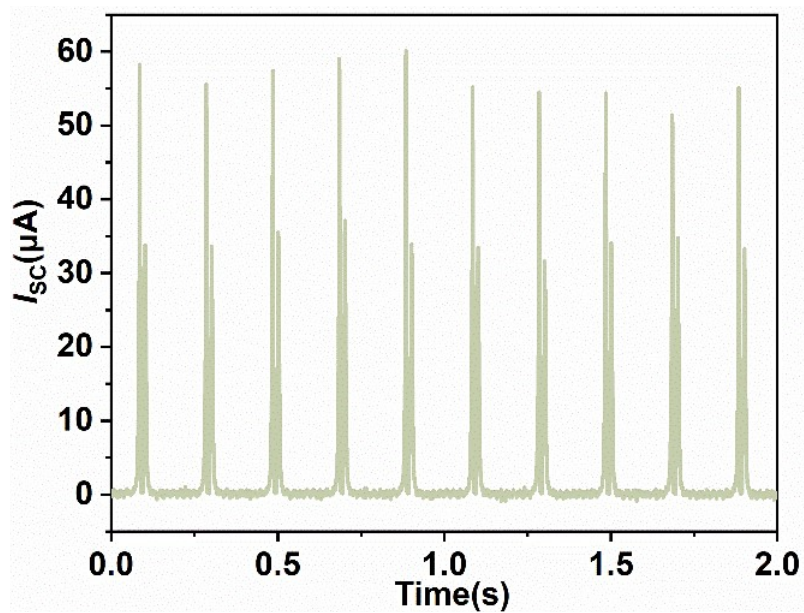


Fig. S19 I_{sc} of Cd-MT through a rectifier bridge.

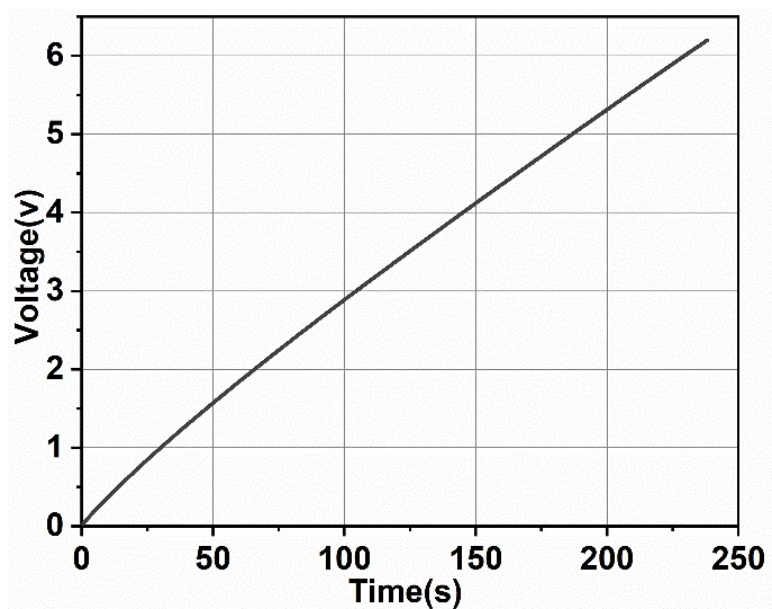


Fig. S20 The charging of 100 μF capacitor using Cd-MT at 5Hz.

Table S1 Crystallographic data and structure refinement details for Cd-MOF.

Compound	Cd-MOF
Formula	C ₂₂ H ₁₄ N ₂ O ₈ Cd
M _r	546.76
T/K	273 K
λ (Mo-Kα)/Å	0.71073
Crystal system	Triclinic
Space group	P2 ₁ /c
a/Å	4.6802(7)
b/Å	15.507(2)
c/Å	12.8345(17)
α (deg)	90
β (deg)	93.757(5)
γ (deg)	90
V (Å ³)	929.5(2)
Z	2
D _{calcd} (g cm ⁻³)	1.954
F(000)	544.0
μ (mm ⁻¹)	1.235
R ₁ (I > 2σ(I))	0.0398
wR ₂ (I > 2σ(I))	0.1091
$R = [\sum F_0 - F_c / \sum F_0], R_w = \sum_w [F_0^2 - F_c^2 ^2 / \sum_w (F_w ^2)^2]^{1/2}$	

Table S2 Selected bond lengths (\AA) and bond angles (deg) for Cd-MOF crystal structure description.

Cd-MOF			
Cd1—O2	2.233 (3)	Cd1—O3ii	2.327 (3)
Cd1—O4i	2.279 (3)	O2iii—Cd1—O4i	92.62 (11)
O4i —Cd1—O3ii	94.81 (11)	O2—Cd1—O4i	87.38 (11)
O4iv—Cd1—O3ii	85.19 (11)	O2iii—Cd1—O4iv	87.38 (11)
O2iii—Cd1—O3v	86.01 (11)	O2—Cd1—O4iv	92.62 (11)
O2—Cd1—O3v	93.99 (11)	O2iii—Cd1—O3ii	93.99 (11)
O4i —Cd1—O3v	85.19 (11)	O2—Cd1—O3ii	86.01 (11)
O4iv—Cd1—O3v	94.81 (11)		
#1 x+1, -y+1/2, z-1/2; #2 -x+2, y+1/2, -z+1/2;			
Symmetry codes: #3 -x+2, -y+1, -z; #4 -x+1, y+1/2, -z+1/2; #5 x, -y+1/2, z-1/2			